IOSR Journal of Mathematics (IOSR-JM)
e-ISSN: 2278-0661,p-ISSN: 2278-8727, Volume 20, Issue 1, Ser. 2 (Jan. – Feb. 2024), PP 01-13
www.iosrjournals.org

Mixed Convective Flow Of Casson Nanofluid In A Vertical Porous Plate With Slip And Temperature Jump Condition

O.A. Ajala[1]. , S.D. Ogundiran[1*], S.O. Sangoniyi[2]
[1]*department Of Pure And Applied Mathematics, Ladoke Akintola University Of Technology, Ogbomoso, Oyo State, Nigeria*
[2]*department Of Mathematics And Computing Science Education, Emmanuel Alayande University Of Education, Oyo, Nigeria*

Abstract
The need to improve the efficiency of industrial based materials and enhances its thermal conductivity has been on increase, this is as a result of the interest in increasing output. Thus, viscous non-Newtonian fluids conveying nanoparticles could serve as a material to meet the engineering and industrial demand for an enhanced productivity, this as apply in electronic gadgets, technology devices, biomedical sciences and others. As such, this study investigated mixed convective steady flow of Casson nanofluid in vertical porous plate with slip and temperature jump boundary conditions. The solution to the dimensionless formulated model is offered via shooting scheme coupled with Runge Kutta method. The sensitivity of the entrenched pertinent dynamical terms on the flow characteristics are examined, and the computed outcomes are demonstrated in graphs and in tabular presentation. The investigation outcomes revealed that the propagation of tiny particle in based fluid enhanced thermal conductivity. Also, the flow rate reduced corresponding to an increase in Hartmann number and material term. The results obtained from this study can be used in engineering, manufacturing and other field of sciences and technologies.

Keywords: *Mixed convection; Casson nanofluid; Porous medium; Velocity slip; Temperature jump*

Date of Submission: 20-01-2024 Date of Acceptance: 30-01-2024

I. Introduction

In recent decades of curious and progressive research, scholars in the domains of science and engineering with particular interests in fluids that enhance heat and mass have paid close attention to the development of a new kind of fluid known as nanofluids [1]. It has been discovered by [2] that the inclusion of nanoparticles improves the fluid's thermophysical characteristics and causes a large improvement in heat transmission. Due to the usefulness of nanotechnology in many areas of manufacture and production, including engineering, energy technologies and medicine, the optimal rate of development in this field has drawn more attention as explained by [3]. The laminar boundary layer flow of an electrically conducting Casson fluid caused by a horizontal perforated sheet that is linearly contracting and expanding with mass transpiration was investigated by [4]. The flow was also subjected to circumstances of Navier's slip and second-order slip in the presence transverse magnetic field applied in the system. The non-Newtonian flow under study follows the Casson model-driven flow's rheological equation. By making use of the proper similarity transformations, the partial differential equations regulating the boundary layer flow were analytically represented and reduced to a nonlinear boundary value problem in ordinary differential equations. The sensitivity parameters were discovered to be functions of the similarity solution. Such a solution was either unique, or dual solutions exist in a region defined by the mass transfer induced slip parameter. The results obtained show that an increase in the magnetic parameter resulting in expansion of the unique solution region and contraction of the dual solution region for the flow due to the induced Lorentz force. In the unique solution region, an increase in magnitudes of mass suction induced slip and the first/second-order slip parameters result in a reduction of the wall shear stress in the shrinking sheet, while the wall shear stress with mass suction increases with the Casson and the magnetic effects. [5] considered motion of temperature dependent viscosity and thermal conductivity of steady incompressible laminar free convective (MHD) non-Newtonian Casson fluid flow over an exponentially stretching surface with exponentially decaying internal heat generation, slip flow and convective heating condition. It was assumed that natural convection is induced by buoyancy and exponentially decaying internal heat generation across the space with convective boundary and velocity slip. The derived ordinary differential equations were solved numerically using the MATLAB bvp4c solver. A parametric study was performed to illustrate the influence of Prandtl number, Casson

parameter, temperature dependent viscosity, temperature dependent thermal conductivity, Magnetic parameter , biot number and velocity slip on the fluid velocity and temperature profiles within the boundary layer. The flow controlling parameters were found to have a great effect on the resulting flow profiles. [6] examined casson fluid flow over a vertical porous surface with chemical reaction in the presence of magnetic field. Similarity analysis was used to transformed the system of partial differential equations reducing the flow problem into ordinary differential equations. The reduced system of equations was solved using the Newton Raphson shooting method alongside the Fourth-order Runge-Kutta algorithm. The results were presented graphically and in tabular form for various controlling parameters.

A research on convective transport in nanofluids where some slip mechanisms capable of producing a relative velocity between the base fluid and the nanoparticles were considered and only Brownian diffusion and thermophoresis were found to be the important ones. It was also observed that nanoparticles move homogeneously with the fluid in the presence of eddies which are turbulent were considered by [7]. [8] investigated the effects of viscous dissipation, suction, thermal diffusion and thermal radiation on the boundary layer flow of nanofluids over a permeable moving flat plate. Runge-Kutta-Fehberg method with the shooting technique was employed as a numerical method for the analysis. A comparative study of the results obtained with previously published work in a limiting sense showed a viable agreement. The boundary layer flow of nanofluid over an unsteady stretching surface in the presence of thermal radiation was examined by [9]. Shooting method with Runge- Kutta-Fehberg scheme was used to numerically analyse the flow scenario. The heat transfer rate at the surface was observed to increase with an increase in the Brownian motion but reduce for thermophoresis. [10] studied hydromagnetic transport phenomena from a stretching or shrinking nonlinear nanomaterial sheet with Navier slip and convective heating: a model for bio-nano-materials processing. The transformed equations were solved using Runge-Kutta-Fehberg fourth fifth order implemented on Maple software and the result depicted that the magnetic parameter reduced the velocity but enhanced the temperature. [11] worked on the effects of nanoparticles on non-Darcy mixed convective transfer of heat within nanofluids over a stretching and shrinking wedge. A solution to the equations of the flow was obtained using fourth order Runge-Kuttamethod along with shooting technique. The result showed that friction factor reduced with an increase in the nanoparticle concentration while the rate of heat transfer increased with it. [12] analysed the computational analysis for bio-convection of microorganisms in Prandtl nanofluid DarcyForchheimer flow across an inclined sheet. Runge-Kutta method alongside shooting technique were used to obtain the solution which revealed that the velocity declined with an increase in the porosity parameter. [13] embarked on a numerical study of flow and heat transfer of a nanofluid past a vertical cone. The obtained equations were solved by Galerkin method with the basis of Legendre functions. Using higher values of volume fraction led to an enhancement of the mechanical behaviour at the surface of the fluid, thereby enhancing the cooling process within the flow. A numerical studied of Casson nanofluid past horizontal stretching surface with magnetic effect and Joule heating was presented by [14]. Slip and thermal convective boundary conditions are considered in the study. A numerical technique of Keller box is applied to the nonlinear ODEs which are obtained by applying the similarity transformation to the nonlinear partial differential equations. The magnetic field and Joule heating effects were observed graphically. It was noted that Nusselt number declines whereas Sherwood number rises by increasing Eckert number. The impact of increasing Hartman number resulted in the decrease of both Sherwood and Nusselt number. The combined effects of Dufour and Soret on the heat and mass transfer in a Casson nanofluid flow over an unsteady stretching sheet with thermal radiation and heat generation. The effects of partial slip on the velocity at the boundary, convective thermal boundary condition, Brownian and thermophoresis diffusion coefficients on the concentration boundary condition were investigated by [15]. The model equations were solved using the spectral relaxation method. The results show that the fluid flow, temperature and concentration profiles were significantly influenced by the fluid unsteadiness, the Casson parameter, magnetic parameter and the velocity slip. The effect of increasing the Casson parameter was to suppress the velocity and temperature growth. An increase in the Dufour parameter reduces the flow temperature, while an increase in the value of the Soret parameter causes increase in the concentration of the fluid. Again, increasing the velocity slip parameter reduces the velocity profile whereas increasing the heat generation parameter increases the temperature profile. A validation of the work is presented by comparing the current results with existing literature.

The effects of combined variable viscosity and thermal conductivity, nonlinear radiation and non-Darcian porous medium on a boundary layer MHD Casson nanofluid flow over a vertical flat plate with convective heating and velocity slip boundary conditions was investigated by [16]. The governing transport nonlinear partial differential equations and the boundary conditions were non-dimensionalized. The resulting system of coupled partial differential equations is then reduced to a set of coupled nonlinear ordinary differential equations using similarity transformation. Galerkin weighted residual method (GWRM) was then employed to solve the resulting set of equations. Numerical results were obtained for dimensionless velocity, temperature and nanoparticle volume fraction (nanoparticle concentration). It was found that the velocity increases, while both temperature and nanoparticle volume fraction decrease with increased values of variable thermal conductivity

and viscosity. Comparisons were carried out with published data in the literature thereby validating the numerical results. An excellent agreement is observed. Furthermore, this present study can find applications in the process involving nanofluid operations. [17] studied how to develop a dynamical system for the magnetohydrodynamic (MHD) flow of an electrically conducting Casson nanofluid on exponentially shrinking and stretching surfaces, in the presence of a velocity and concentration slip effect, with convective boundary conditions. The results revealed that the temperature of the fluid increases with the extended values of the thermophoresis parameter, the Brownian motion parameter, and the Hartmann and Biot numbers, for both solutions. The presence of dual solutions depends on the suction parameter. In order to indicate that the first solution is physically relevant and stable, a stability analysis had been performed. [19] examined MHD Boundary Layer Flow Past an Exponentially Stretching Sheet with Darcy-Forchheimer Flow showed that the rate of heat transfer increased with an increase in the permeability parameter.

[24] explored natural convective non-Newtonian Casson fluid flow in a porous medium with slip and temperature boundary conditions. Inspired by the aforementioned research, we attempted to examine mixed convective flow of Casson nanofluid in a vertical porous plate with slip and temperature jump boundary conditions in this publication. In this study, the motion of nanoparticles in a fluid flow was taken into account along with thermophoresis and Brownian motion. This study's innovation is the way relevant parameters affect mixed convective flow of Casson nanofluid in a vertical porous plate under slip and temperature jump conditions. Using the shooting scheme alongside fourth-order Runge Kutta method, the derived non-linear ordinary differential equations were solved. The numerical findings for velocity, temperature and concentration are presented in plots. The findings of this study make a substantial contribution to our knowledge and complement earlier research for applications in fields like biomedical engineering and heat transfer.

II. Formulation of the problem

Consider a Casson nanofluid flow of a mixed convective incompressible, electrically conducting, hydromagnetic in vertically porous medium. The plates were subjected to steady periodic heating which leads to temperature and concentration gradient of the fluid, thereby setting the fluid in motion. From this assumption, one porous plate (y = -h) was subjected to suction while the other porous plate (y = +h) was subjected to injection. The low wall was heated with slip and temperature jump. The porous plate was taken vertically parallel to the x-axis at y = $\pm$ h.

For Casson fluid, the constituting equations of isotropic and oscillatory flow can be expressed as [21, 22 ,23].

$$\tau_{ij} = \begin{cases} \left(\mu_B + P_y / \sqrt{2\pi_c}\right) 2e_{ij}, & \pi_c > \pi \\ \left(\mu_B + P_y / \sqrt{2\pi}\right) 2e_{ij}, & \pi > \pi_c \end{cases} \tag{1}$$

Where τ_{ij} is the $(i,j)^{th}$ component of the stress tensor, e_{ij} is the $(i,j)^{th}$ component of the strain rate tensor, $\pi = e_{ij}^2$ denotes the product of the component of the strain rate tensor, π_c is the critical value of this product based on the non-Newtonian fluid, μ_B is the plastic dynamic viscosity of the non-Newtonian fluid, P_y is the yield stress of the fluid.

The modified governing equations are [24].

$$\frac{\partial u}{\partial x} + \frac{\partial v}{\partial y} = 0 \tag{2}$$

$$\frac{\partial u'}{\partial t'} - v_0 \frac{\partial u'}{\partial y'} = \nu_f \left(1 + \frac{1}{c}\right) \frac{\partial^2 u'}{\partial y'^2} + g\beta_t (T - T_0) + g\beta_c (C - C_0) - \frac{\sigma_f B_0^2 u'}{\rho_f} - \nu_f \left(1 + \frac{1}{c}\right) \frac{u'}{K} \tag{3}$$

$$\frac{\partial T}{\partial t'} - v_0 \frac{\partial T}{\partial y'} = \frac{k_f}{(\rho C_p)_f} \frac{\partial^2 T}{\partial y'^2} + \frac{Q_0}{(\rho C_p)_f} (T_0 - T) - \frac{1}{(\rho C_p)_f} \frac{\partial q_r}{\partial y'} + \frac{\sigma_f B_0^2 u'^2}{(\rho C_p)_f}$$

$$+ \frac{\mu_f}{(\rho C_p)_f} \left(1 + \frac{1}{c}\right) \left(\frac{\partial u'}{\partial y'}\right)^2 + \frac{\mu_f}{(\rho C_p)_f} \left(1 + \frac{1}{c}\right) \frac{u'^2}{K} + \tau \left[D_B \frac{\partial C}{\partial y} \frac{\partial T}{\partial y} + \frac{D_T}{T_m} \left(\frac{\partial T}{\partial y}\right)^2 \right] \tag{4}$$

$$\frac{\partial C}{\partial t} - v_0 \frac{\partial C}{\partial y} = D_B \frac{\partial^2 C}{\partial y^2} + \frac{D_T}{T_m} \left(\frac{\partial^2 T}{\partial y^2}\right) \tag{5}$$

with initial condition

$$u'(t',y')=0, T(t',y')=0, C(t',y')=0 \quad at \quad t'=0 \tag{6}$$

For rarefied flow with temperature jump, the appropriate boundary condition can written as

$$u'(t',y')=\frac{2-\xi}{\xi}\gamma\frac{\partial u'}{\partial y'} \tag{7}$$

$$T(t',y')=T_1+T_2\cos(\omega t)+\frac{2-\sigma_t}{\sigma_t}\frac{2\varphi}{\varphi+1}\frac{\gamma}{\Pr}\frac{\partial T}{\partial y'},\ y'=-h \quad at \ \ t'>0 \tag{8}$$

$$C(t',y')=C_1+C_2\cos(\omega t)+k_c\frac{\partial C}{\partial y'} \quad , \quad y'=-h \quad at \quad t'>0 \tag{9}$$

The non moving wall and isothermal condition gives

$$u'(t',y')=0, T(t',y')=T_1+T_2\cos(\omega t), \quad y'=h \quad at \quad t'>0 \tag{10}$$

$$C(t',y')=C_1+C_2\cos(\omega t), \quad y'=h \quad at \quad t'>0 \tag{11}$$

By using Roseland approximation, the radiative heat flux term is given by

$$q_r=-\frac{4\gamma'}{3\alpha'}\frac{\partial T^4}{\partial y'} \tag{12}$$

where γ' and α' are stefan Boltzman constant and Roseland mean absorption coefficient. Assuming The difference with the flow are abundantly small such that T^4 can be expressed as liner function of the Temperature. It is acheived by expanding T^4 in a Taylor series about T and neglecting the higher order terms, we get

$$T^4=(4T_1)^3T-3T_1^4 \tag{13}$$

Substituting equation (12) and (13) into equation (4) gives

$$\frac{\partial T}{\partial t'}-v_0\frac{\partial T}{\partial y'}=\frac{k_f}{(\rho C_p)_f}\frac{\partial^2 T}{\partial y'^2}+\frac{Q_0}{(\rho C_p)_f}(T_0-T)-\frac{16\gamma' T_1^3\partial^2 T}{3\alpha'\partial y'^2}+\frac{\sigma_f B_0^2 u'^2}{(\rho C_p)_f}$$

$$+\frac{\mu_f}{(\rho C_p)_f}\left(1+\frac{1}{c}\right)\left(\frac{\partial u'}{\partial y'}\right)^2+\frac{\mu_f}{(\rho C_p)_f}\left(1+\frac{1}{c}\right)\frac{u'^2}{K}+\tau\left[D_B\frac{\partial C}{\partial y}\frac{\partial T}{\partial y}+\frac{D_T}{T_m}\left(\frac{\partial T}{\partial y}\right)^2\right] \tag{14}$$

III. Model transformation

Solving equations (3) to (14), then equations (15) to (17) were employed to split the velocity, temperature and concentration into steady and periodic part, respectively according to [24], as follows:

$$u'(t',y')=\frac{h^2}{\nu}\left((T_1-T_0)A(y)+T_2B(y)e^{i\omega t}\right) \tag{15}$$

$$T'(t',y')=T_0+(T_1-T_0)F(y)+T_2G(y)e^{i\omega t} \tag{16}$$

$$C'(t',y')=C_0+(C_1-C_0)M(y)+C_2Z(y)e^{i\omega t} \tag{17}$$

Where A(y), F(y), M(y) depicts the steady parts and B(y), G(y), Z(y) for the periodic parts of the velocity, temperature and concentration, respectively. The dimensionless quantities used are

$$y=\frac{y'}{h},\ S_t=\frac{i\omega}{\nu},\ P_r=\frac{k_f}{(\rho C_p)_f\nu_f},\ \delta=\frac{Q_0}{k_f},\ c=\frac{\mu_B\sqrt{2\pi}}{P_y},\ K_n=\frac{\lambda}{h}\left(\frac{2-\sigma_t}{\sigma_t}\right)\frac{2\varphi}{\varphi+1}$$

$$Da=\frac{k}{h^2},\ \gamma=\frac{(2-\xi)\lambda}{\xi h},\ H=\frac{\sigma_f B_0{}^2}{\mu_f},\ \beta=\frac{1}{Da},\ N=\frac{4\sigma T_1^3}{\alpha k_f},\ E_c=\frac{h^4}{C_p\nu_f}\rho(T_1-T_0)$$

$, \ Nb = \frac{\tau D_B (C_1 - C_0)}{\nu_f}, \ Nt = \frac{\tau D_T (T_1 - T_0)}{T_m \nu_f}$

$\alpha_f = \frac{k_f}{(\rho C_p)_f}, \ Le = \frac{\alpha_f}{D_B}, \ \delta_1 = \frac{k_c h^2}{\nu_f}, \ S = \frac{v_0}{\nu_f}, \ \lambda = \frac{g\beta_t}{h^2}, \ Q_1 = \frac{\beta_c (C_1 - C_0)}{\beta_t (T_1 - T_0)}$ `$Q_2 = \frac{\beta_c C_2}{\beta_t T_2}$,

$Sc = \frac{v_0}{D_B}, \ \left(\frac{Nt}{Nb}\right) = \frac{D_T (T_1 - T_2)}{T_m D_B (C_1 - C_2)}$, (18)

Applying equation (15) to (17) into the equations (3) to (5) and taking the order of $e^{i\omega t}$, non-linear coupled ordinary differential equations was obtained as:

$$\left(1+\frac{1}{c}\right)A''(y) + SA'(y) - \left(H^2 + \left(1+\frac{1}{c}\right)\beta\right)A(y) + \lambda\left(F(y) + Q_1 M(y)\right) = 0 \quad (19)$$

$$\left(1+\frac{4}{3}N\right)F''(y) + \Pr SF'(y) + \Pr\left(Nb\,M'(y) + Nt\,F'(y)\right)F'(y) + \delta F(y)$$

$$+ \Pr Ec\left(H^2 + \beta\left(1+\frac{1}{c}\right)\right)(A(y))^2 + \Pr Ec\left(A'(y)\right)^2 = 0 \quad (20)$$

$$\left(1+\frac{1}{c}\right)B''(y) + SB'(y) - \left(S_t + H^2 + \left(1+\frac{1}{c}\right)\beta\right)B(y) + \lambda\left(G(y) + Q_2 Z(y)\right) = 0 \quad (21)$$

$$\left(1+\frac{4}{3}N\right)G''(y) + \Pr S\,G'(y) + 2Nt\Pr G'(y) + Nb\Pr\left(M'(y)G'(y) + Q_3 F'(y)Z'(y)\right) - \left(\Pr S_t + \delta\right)G(y)$$

$$+ 2\Pr Ec\left(H^2 + \left(1+\frac{1}{c}\right)\beta\right)A(y)B(y) + 2\Pr Ec\left(1+\frac{1}{c}\right)A'(y)B'(y) = 0 \quad (22)$$

$$M''(y) + ScM'(y) + \left(\frac{N_t}{N_b}\right)F''(y) = 0 \quad (23)$$

$$Z''(y) + Sc(SZ'(y) - S_t Z(y)) + \left(\frac{Nt}{Nb}\right)G''(y) = 0 \quad (24)$$

These equations were subjected to the boundary conditions highlighted in equation (25)

$$A(-1) = \gamma A'(-1), A(1) = 0$$
$$F(-1) = 1 + \frac{K_n}{P_r}F'(-1), F(1) = 1$$
$$M(-1) = 1 + \delta_1 M'(-1), M(1) = 1$$
$$B(-1) = \gamma B'(-1), B(1) = 0$$
$$G(-1) = 1 + \frac{K_n}{P_r}G'(-1), G(1) = 1$$
$$Z(-1) = 1 + \delta_1 Z'(-1), Z(1) = 1 \quad (25)$$

Skin friction , $C_f = \left(1+\frac{1}{c}\right)\frac{dB(y)}{dy}$, Nusselt number, $Nu = \left(1+\frac{4}{3}N\right)\frac{dG(y)}{dy}$ and the mass transfer rate $Sh = \frac{dZ(y)}{dy}$ at the walls.

IV. Numerical procedure

The system of second order non-linear ordinary differential equations (19) to (24) is transformed into a set of first-order ordinary differential equations by substituting the following;

Let $a_1 = A$, $a_2 = A'$, $a_3 = B$, $a_4 = B'$, $a_5 = F$, $a_6 = F'$, $a_7 = G$, $a_8 = G'$, $a_9 = M$, $a_{10} = M'$, $a_{11} = Z$, $a_{12} = Z'$ (26)

$$a_2' = \frac{\left(H^2 + \beta\left(1+\frac{1}{c}\right)\right)a_1 - \lambda\left(a_5 + Q_1 a_9\right) - Sa_2}{\left(1+\frac{1}{c}\right)} \tag{27}$$

$$a_6' = \frac{-1}{\left(1+\frac{4}{3}N\right)}\left(\Pr S a_6 + \delta a_5 + \Pr Ec\left(H^2 + \beta\left(1+\frac{1}{c}\right)\right)a_1^2 + \Pr Eca_2^2 + \Pr\left(Nba_{10} + \Pr Nta_6\right)a_6\right) \tag{28}$$

$$a_{10}' = -Sca_{10} - \left(\frac{Nt}{Nb}\right)a_6' \tag{29}$$

$$a_4' = \frac{\left(S_t + H^2 + \beta\left(1+\frac{1}{c}\right)\right)a_3 - \lambda\left(a_7 + Q_2 a_{11}\right) - Sa_4}{\left(1+\frac{1}{c}\right)} \tag{30}$$

$$a_8' = \frac{-1}{\left(1+\frac{4}{3}N\right)}\left(\begin{array}{l}\Pr S a_8 - \Pr S_t a_7 - \delta a_7 + 2H^2 \Pr Eca_1 a_3 + 2\Pr Ec\left(1+\frac{1}{c}\right)a_2 a_4 \\ + 2\Pr Ec\beta\left(1+\frac{1}{c}\right)a_1 a_3 + Nb\Pr\left(a_8 a_{10} + Q_3 a_6 a_{12}\right) + 2\Pr Nta_6 a_8\end{array}\right) \tag{31}$$

$$a_{12}' = -Sc\left(Sa_{12} - S_t a_{11}\right)a_{10} - \left(\frac{Nt}{Nb}\right)a_8' \tag{32}$$

Subject to the boundary conditions below;

$$a_1(-1) = \gamma\, a_2(-1),\ a_1(1) = 0,\ a_5(-1) = 1 + \frac{kn}{\Pr}a_6(-1),\ a_5(1) = 1,$$

$$a_9(-1) = 1 + \delta_1\, a_{10}(-1),\ a_9(1) = 1\ a_3(-1) = \gamma\, a_4(-1),\ a_3(1) = 0,$$

$$a_7(-1) = 1 + \frac{kn}{\Pr}a_8(-1),\ a_7(1) = 1,\ a_{11}(-1) = 1 + \delta_1\, a_{12}(-1),\ a_{11}(1) = 1$$

The reduced initial value equations (26) to (32) are to be solved. The shooting technique is employed to guess the unknown points $a_2(-1) = r_1, a_4(-1) = r_2, a_6(-1) = r_3, a_8(-1) = r_4, a_{10}(-1) = r_5,$ $a_{12}(-1) = r_6$ until the boundary condition is satisfied. The fourth-order Runge-Kutta integration approach was used to solve the obtained differential equations, and numerical computations are carried out with the Maple 18 software package. To establish the correctness of the presented results and determine the accuracy of the adopted numerical method, a comparison of result with the existing one is carried out as presented in Table 1

Table 1: Comparison of results for $G(y)$ with previous works for: S =1, St =1, β = 0, H = 0, δ =1, $\Pr = 1$, $N = 15$, $Kn = 0$, $\gamma = 0$, $Ec = 0$, $\lambda = 0$, $Q_1 = 0$.

y	Titiloye(2018)	Obalalu (2020)	Present work
-1.0	0.999999	0.999999	1.000000
-0.8	0.799521	0.799521	0.799521
-0.6	0.685677	0.685677	0.685677
-0.4	0.626398	0.626398	0.626398
-0.2	0.605794	0.605794	0.605794
0	0.602555	0.602555	0.602555
0.2	0.646716	0.646716	0.646716
0.4	0.700614	0.700614	0.700614
0.6	0.775963	0.775963	0.775963

0.8	0.874578	0.874578	0.874578
1.0	0.999999	0.999999	1.000000

V. Results and discussion

In this section, the impact of different thermophysical dynamical terms on unsteady flow regimes was obtained with the aid of plots. It can be observed from Table 2, that the skin friction improved whenever radiation and thermophoresis dynamical term gained values but decreased with an upsurge in magnetic and permeability dynamical terms. Also an increase in thermophoresis decreased the Nusselt number while it declined with an upsurge in radiation and magnetic dynamical terms. Sherwood number improved with an upsurge in thermophoresis but decreased with an upsurge in radiation and porous dynamical terms.

Table 2: Effect of different thermo physical dynamical terms on the Shear stress, the heat transfer rate and the rate of mass transfer at the surface of the plate for $Kn = 0.005, S_t = \delta = Sc = \gamma = 1.0,$ $c = Q_1 = Q_2 = 0.1,\ \Pr = 0.71.$

								(C_f)	-(Nu)	-(Sh)
.1	.6	.5		.2	.2	.2	.0	0 .0297	0.3 227	0.542 3
.5	.6	.5		.2	.2	.2	.0	0 .1213	0.3 027	0.558 8
.0	.6	.5		.2	.2	.2	.0	0 .1284	0.3 012	0.559 9
.1	.0	.5		.2	.2	.2	.0	0 .0318	0.0 732	0.747 6
.1	.0	.5		.2	.2	.2	.0	0 .0353	0.3 614	1.104 7
.1	.6	.5		.2	.2	.2	.0	0 .0262	0.3 090	0.553 6
.1	.6	.0		.2	.2	.2	.0	0 .0168	0.2 727	0.583 4
.1	.6	.5		.2	.2	.2	.0	0 .0314	0.1 197	0.709 5
.1	.6	.5		.2	.2	.2	.0	0 .0315	0.1 064	0.720 4
.1	.6	.5		.0	.2	.2	.0	0 .0298	0.3 383	0.651 9
.1	.6	.5		.5	.2	.2	.0	0 .0300	0.3 862	0.900 5
.1	.6	.5		.2	.4	.2	.0	0 .0296	0.3 229	0.674 5
.1	.6	.5		.2	.6	.2	.0	0 .0296	0.3 228	0.718 6
.1	.6	.5		.2	.2	.4	.0	0 .0299	0.3 306	0.262 6
.1	.6	.5		.2	.2	.6	.0	0 .0301	0.3 384	0.032 4
.1	.6	.5		.2	.2	.2	.0	0 .0217	0.2 915	0.567 9
.1	.6	.5		.2	.2	.2	.0	0 .0171	0.2 736	0.582 6

In this section, the significance of the numerous thermophysical dynamical terms on steady flow regimes are obtained with the help of graphs.

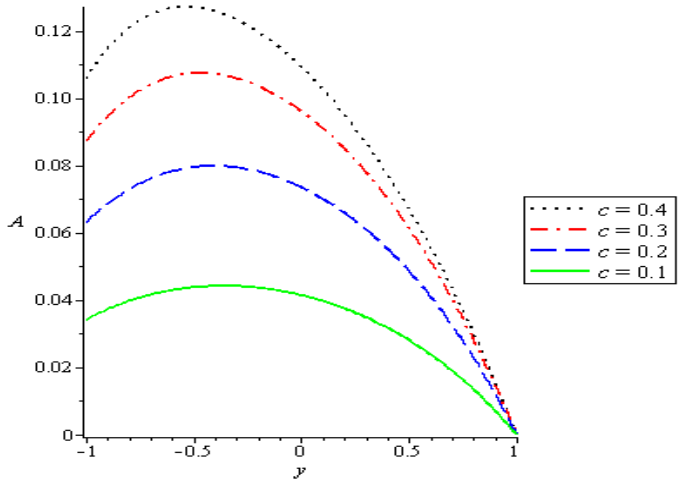

Fig 1: Velocity profile for different values casson parameter

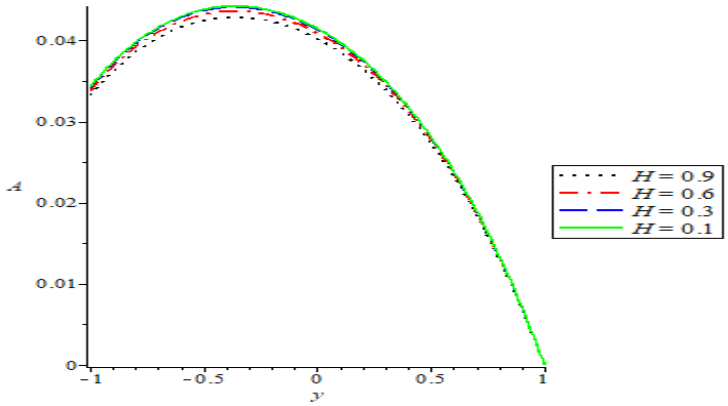

Fig 2: Velocity profile for different values of Hartmann number

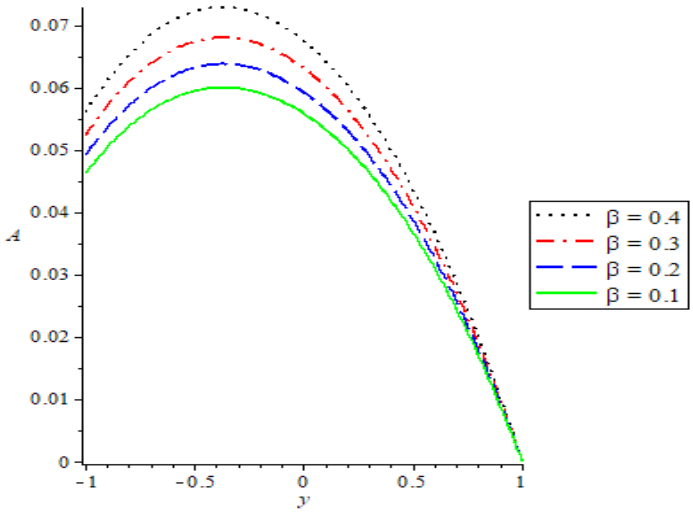

Fig 3: Velocity profile for different values of porous parameter

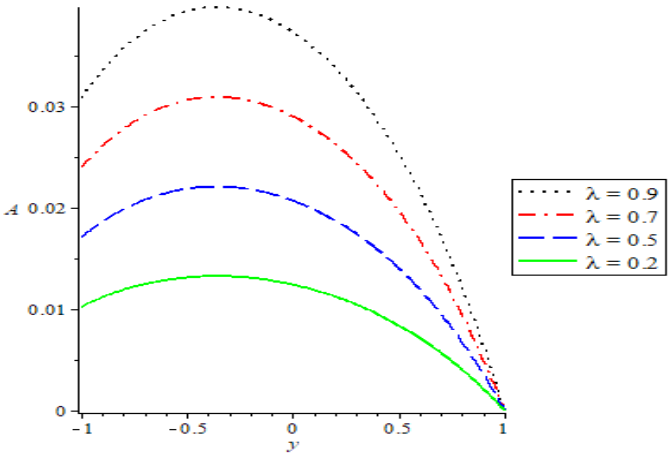

Fig 4: Velocity profile different value Convective parameter

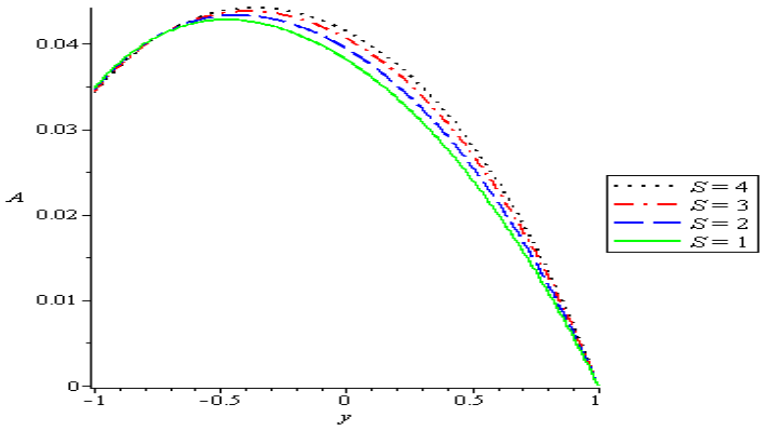

Fig 5: Velocity profile for different value of suction parameter

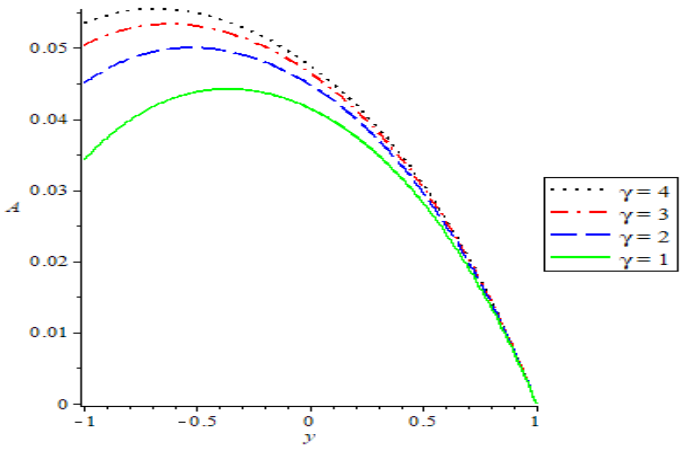

Fig 6: Velocity profile for different Slip parameter

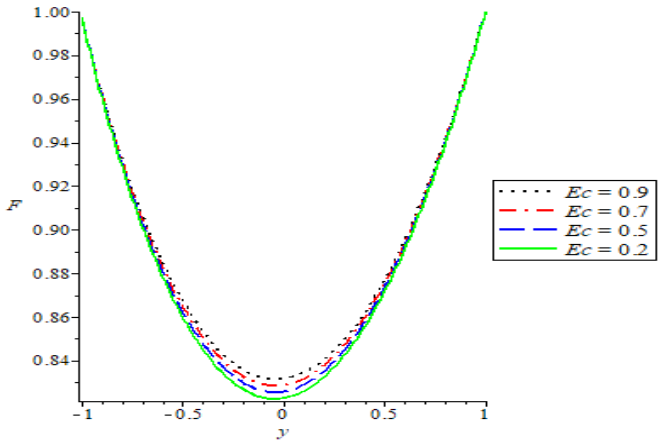

Fig 7: Temperature profile for different values of Eckert Number

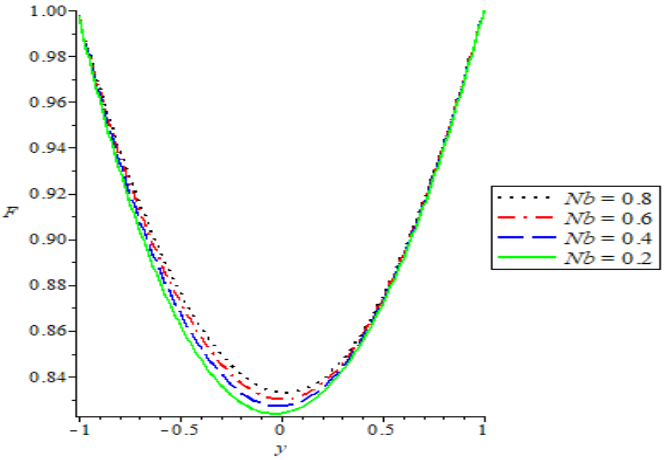

Fig 8: Temperature profile for different values of Brownian motion parameter

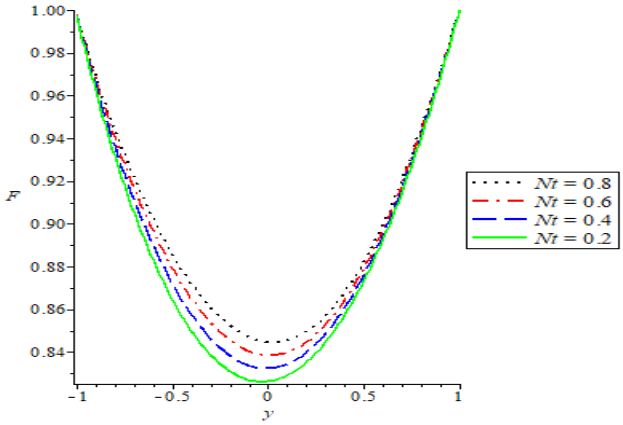

Fig 9: Temperature profile for different values of Thermophoresis parameter

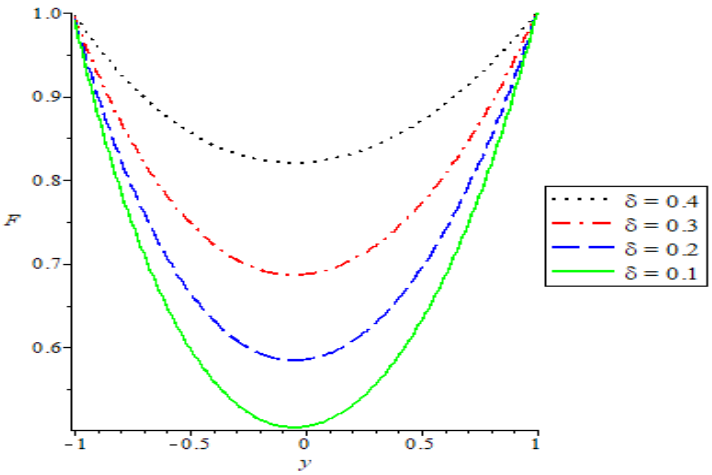

Fig 10: Temperature profile for different heat generation parameter

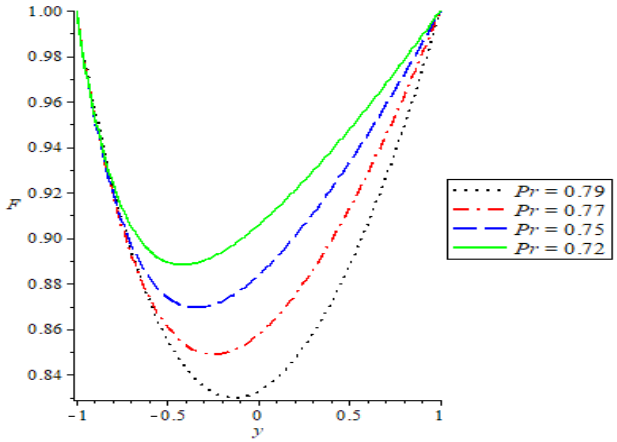

Fig 11: Temperature profile for different Prandtl Number

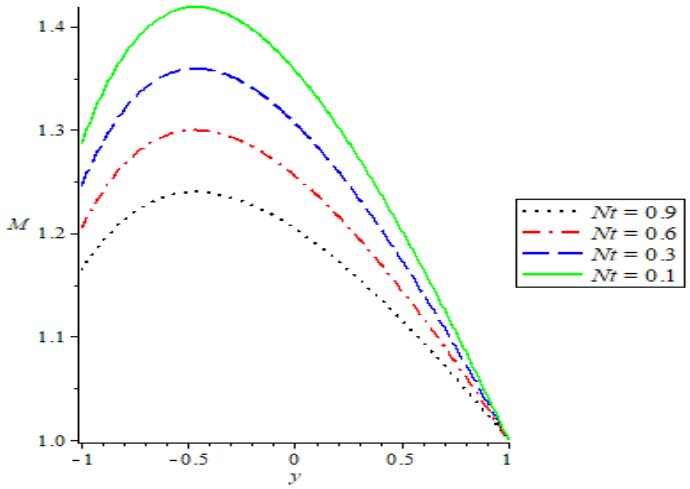

Fig 12: Concentration profile for different Thermophoresis parameter

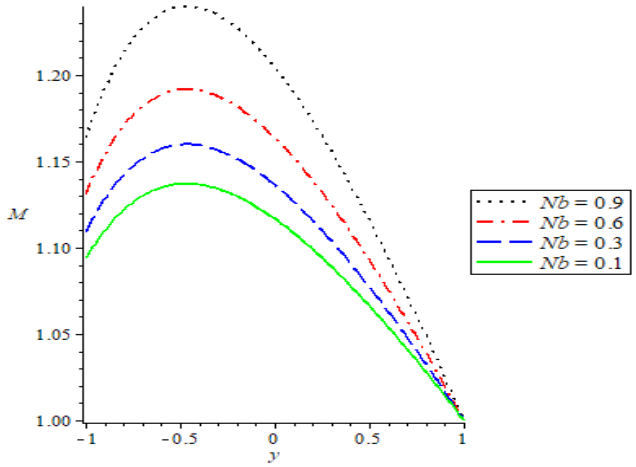

Fig 13: Concentration profile for different Brownian motion parameter

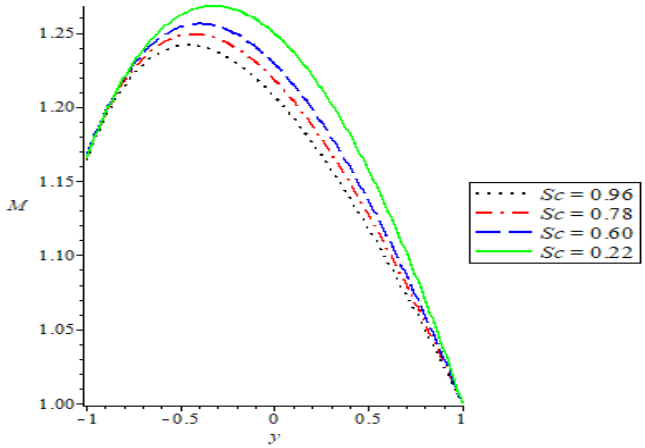

Fig 14: Concentration profile for different Schmidt number

Figure 1-14 show the response of velocity, temperature and concentration profile against space for the variation of sensitivity parameters in the steady flow regime. In Figure 1, the effect of Casson parameter on fluid velocity is observed. It is discovered that an increase in Casson parameter increases the fluid velocity but reduces at the wall. It has been discovered that adequate Casson nanofluid dissolves the response of the non-Newtonian action. This suggests that the pure fluid will act as a Newtonian fluid. However, the Casson nanofluid flow for the boundary plate thickness is higher as compared to the Newtonian fluid. This can be attributed to the plasticity of Casson nanofluid. It is noted that a rise in the value of Casson nanofluid tends to reduce the plasticity of the fluid to rise. Figure 2 depicts the effect of magnetic field intensity on the Casson nanofluid velocity. It is discovered that an increase in magnetic field intensity tends to reduce the fluid flow due to the existence Lorentz force i.e opposing force which retard the fluid velocity. Figure 3 represents the impact of porous parameter on Casson nanofluid flow. By implication an increase in the porosity parameter leads to increase in permeability of the channel thereby enhances the fluid flow. Figure 4 shows the influence of convective parameter on the Casson nanofluid flow. This implies that an increase in convective parameter leads to enhancement of the Casson nanofluid flow. Figure 5 presents the impact suction parameter on the Casson nanofluid flow. It has been discovered that an increase in suction parameter leads to rise in the nanofluid flow. Figure 6 reveals the effect of velocity slip parameter on the Casson nanofluid flow. A rise in the velocity slip parameter consequently enhances the velocity of the fluid flow due to the interaction between the gas molecules. Figure 7 depicts the impact of viscous dissipation on the temperature of Casson nanofluid. It is observed that as the Eckert number rises it enhance the temperature of the fluid flow. By implication, as Eckert number increases more thermal energy is supplied to increase the fluid temperature, an increase in viscous dissipation in terms of Eckert number enhances the fluid temperature. Figure 8 exhibits the effect of Brownian motion parameter on the temperature of Casson nanofluid. An increase in Brownian parameter led to increase in temperature profile. As Brownian motion corresponds to random movement of nanoparticles in the fluid. This random movement enhances the nanoparticles collision with fluid molecules and as a result, molecules kinetic energy is converted to thermal energy and hence temperature rises. Figure 9 presents the influence of thermophoresis parameter on the

temperature of the Casson nanofluid flow. An increase in thermophoresis parameter increases the temperature profile. Thermophoresis phenomenon accelerates the particles from the hotter region to cooler region. Consequently, heat moves rapidly from hotter surface to fluid, and hence it increases the temperature of the fluid. Figure 10 depicts impact heat generation parameter on the temperature of the fluid flow. As the heat generation parameter increases temperature profile rise. Figure 11 reflects the influence Prandtl number on the temperature of the Casson nanofluid. An increase in Prandtl number reduces the temperature profile of the fluid. This is as a result of decrease in thermal conductivity of the fluid within the channel. An increase in thermophoresis parameter reduces the concentration profile of the nanoparticles as shown in Figure 12. It is observed that the concentration distributions decrease due to increment in thermophoresis parameter. Figure 13 presents the effect of Brownian motion parameter on the concentration of Casson nanofluid. The temperature increases due to the possibility of more often collision of the particles and the molecules in the fluid which results in the release of heat, reaction is increase which led to increase in concentration distribution. Concentration profile for different values of Schmidt number is presented in Figure 14. It is observed that concentration decreases as Schmidt number increases. Schmidt number is the ratio of the viscous forces to diffusivity; therefore, as such increases species concentration decreases.

VI. Conclusions

In this manuscript, a mathematical model to study mixed convective flow of casson nanofluid in a vertical porous plates with slip and temperature jump boundary condition is presented. The influence of pertinent parameters on the fluid flow, heat and mass transfer characteristics are investigated. The features of flow characteristics are presented by plotting graphs and elucidated in detail. The following conclusions are made:

1. Velocity distribution increases with increasing casson fluid parameter, porosity parameter, convective parameter, slip parameter while it decreases with increasing Hartmann number and Strouhal number.
2. Temperature distribution increases with increasing Eckert number, Thermophoresis parameter, heat generation parameter and Brownian motion parameter while it decreases with increasing Prandtl number.
3. Nanoparticles concentration distribution decreases with increasing Schmidt number and Thermophoresis parameter while it increases with increasing Brownian motion parameter.

REFERENCES

[1]. Rafique, K., Anwar, M.I. And Misiran, M. (2019). Numerical Study On Micropolar Nanofluid Flow Over An Inclined Surface By Means Of Keller-Box. Asian J. Probab. Stat, 4,1-21.
[2]. Singh, J., Vishalakshi, A.B., Mahabaleshwar, U. S And Bognar, G (2022). Mhd Casson Fluid Flow With Navier's And Second Order Slip Due To A Perforated Stretching Orn Shrinking Sheet. Journal.Pone, 17(11): E0276870.
[3]. Radha, G., Reddy, N.B And Gangadhor, K (2017). Slip Flow Of Casson Fluid With Variable
[4]. Thermophysical Properties Along Exponentially Stretching Sheet Under Convective Heating. International Journal Of Mechanics And Solids. 12(2), (2017), Pp 235-256.
[5]. Arthur, E.M., Seini, I.Y. And Bortteir, L.B. (2015). Analysis Of Casson Fluid Flow Over A Vertical Porous Surface With Chemical Reaction In The Presence Of Magnetic Field. Journal Of Applied Mathematics And Physics, 3(2015), 713-723.
[6]. Buongiorno, J. (2006).Convective Transport In Nanofluids, Journal Of Heat Transfer, 128, 240-250.
[7]. Motsumi, T.G And Makinde, O.D. (2012). Effects Of Thermal Radiation And Viscous Dissipation On Boundary Layer Flow Of Nanofluids Over A Permeable Moving Flat Plate. Phys. Scr. 86(4). Doi:10.1088/0031-8949/86/04/045003.
[8]. Das, K., Duari, P.R. And Kundu, P.K (2014). Nanofluid Flow Over An Unsteady Stretching Surface In The Presence Of Thermal Radiation, Alexandria Engineering Journal, 53, 737-745.
[9]. Uddin, M.J., Beg, O.A., And Amin, N. (2014). Hydromagnetic Transport Phenomena From A Stretching Or Shrinking Nonlinear Nanomaterial Sheet With Navier Slip And Convective Heating: A Model For Bio-Nano-Materials Processing. Journal Of Magnetism And Magnetic Materials, 368, 252-261.
[10]. El-Dawy, H.S.A.And Gorla R.S.R. (2019). Effects Of Nanoparticles On Non-Darcy Mixed Convective Heat Transfer In Nanofluids Over A Shrinking And Stretching Wedge, Applied Computational Mathematics, 8(4), 70-74.